Quantum-based Super-Resolution Imaging with Multi-Aperture Systems

Nicolas Deshler and Amit Ashok

Wyant College of Optical Sciences, University of Arizona, Tucson AZ, USA

ndeshler@arizona.edu, ashoka@arizona.edu

Abstract: We extend the quantum-based modal imaging framework to multiple apertures. Using simulations we demonstrate that our approach is capable of resolving multiple incoherent point sources well beyond the diffraction limit. © 2023 The Author(s)

1. Introduction

In conventional diffraction-limited imaging systems, the smallest resolvable feature in a scene is inversely proportional to the size of the system aperture. This relationship has been referred to as 'Rayleigh's Curse', as achieving higher resolution incurs the cost of larger optical apertures. A multi-aperture imaging system synthesizes a large monolithic aperture by interfering light from a network of smaller sub-apertures, as commonly employed in radio astronomy. Thus multiple apertures enhance resolution while avoiding many of the technical engineering challenges associated with fabricating a large contiguous focusing element. In this work, we propose a quantum-inspired Spatial Mode Demultiplexing (SPADE) receiver [1] that achieves super-resolution imaging using multiple apertures. We numerically evaluate SPADE's capacity to localize multiple incoherent point sources within a sub-Rayleigh field of view.

2. Theory

2.1. Systems of Identical Circular Apertures and the Density Operator for Constellations

Equation 1 defines the point spread function (PSF) of a multi-aperture system with m identical circular sub-apertures of radius $\delta = d/2$ centered at $\{\vec{h}_\mu = (k_{x_\mu}, k_{y_\mu})\}_{\mu=1}^m$. The Rayleigh limit $\sigma = 2\pi \cdot 1.22 \frac{\lambda}{D}$ is defined in terms of the diameter D of the circle circumscribing the sub-aperture network (Figure 1a-c).

$$\psi_0(\vec{r}) = \frac{J_1(\delta|\vec{r}|)}{\pi|\vec{r}|} \frac{1}{\sqrt{m}} \sum_{\mu=1}^m e^{i\vec{h}_\mu \cdot \vec{r}} \tag{1}$$

A constellation of n incoherent point sources is completely characterized by the object-plane source coordinates $\{\vec{\alpha}_i = (x_i', y_i')\}_{i=1}^n$ and their relative brightness $\{b_i > 0\}_{i=1}^n$ with the constraint $\sum_{i=1}^n b_i = 1$. If an optical system with unit magnification images an arbitrary constellation, the density operator describing the single-photon excitation state of the field at the image plane is given by Equation 2 where $\theta = [\vec{\alpha}_1, b_1, \ldots, \vec{\alpha}_n, b_n]$.

$$\hat{\rho}(\theta) = \sum_{i=1}^n b_i |\psi_0(\vec{\alpha}_i)\rangle\langle\psi_0(\vec{\alpha}_i)| \qquad \text{where} \qquad |\psi_0(\vec{\alpha})\rangle = \iint \psi_0(\vec{r} - \vec{\alpha})|\vec{r}\rangle d^2r \tag{2}$$

2.2. PSF-Adapted Basis for Spatial Mode Demultiplexing

A quantum SPADE measurement consists of two parts: (1) decomposing the optical field at the image plane into a set of orthonormal transverse modes, (2) detecting a single photon in one of the modes. Choosing a set of modes that are well-suited for the estimation task is vital. The PSF-adapted (PAD) basis [2] tailors the modes to the aperture by defining the fundamental mode as the PSF. This renders the basis highly sensitive to small off-axis source displacements. The PAD basis $\{\psi_j(\vec{r})\}$ is constructed by performing Gram-Schmidt orthonormalization on repeated partial derivatives of the PSF in Cartesian coordinates as shown in Equation 3. The expansion of the shifted PSF state in the PAD basis states is given in Equation 4 where A is the total aperture area.

$$\psi_0^{(j)}(\vec{r}) = (\partial_x)^p(\partial_y)^q \psi_0(\vec{r}) \qquad \rightarrow \qquad \psi_j(\vec{r}) = \frac{1}{\sqrt{N_{pq}}} \left[\psi_0^{(j)}(\vec{r}) - \sum_{0 \le j' < j} \left(\iint \psi_{j'}^*(\vec{u}) \psi_0^{(j)}(\vec{u}) d^2u \right) \psi_{j'}(\vec{r}) \right] \tag{3}$$

$$|\psi_0(\vec{\alpha})\rangle = \frac{2\pi}{\sqrt{A}} \sum_{j=0}^{\infty} \psi_j^*(\vec{\alpha}) |\psi_j\rangle \qquad \text{where} \qquad |\psi_j\rangle = \iint \psi_j(\vec{r}) |r\rangle \, d^2r \qquad (4)$$

2.3. Estimation Task

Given K identical copies of the single-photon state $\hat{\rho}(\theta)$, we repeat the same SPADE measurement K times and treat each photon detection as an independent event. In any given measurement, the probability of finding the field in the state $|\psi_j\rangle$ is $p_j(\theta) = \langle \psi_j | \hat{\rho}(\theta) | \psi_j \rangle = \frac{4\pi^2}{A} \sum_{i=1}^{n} b_i |\psi_j(\vec{\alpha}_i)|^2$. Let k_j be the number of times the state $|\psi_j\rangle$ was observed so that $\sum_{j=0}^{\infty} k_j = K$. From this data, our task is to estimate the parameters θ. We do so by finding the maximum likelihood estimator: $\check{\theta} = \underset{\theta}{\text{argmax}} \sum_{j=0}^{\infty} k_j \log(p_j(\theta))$ using the Expectation Maximization (EM) algorithm.
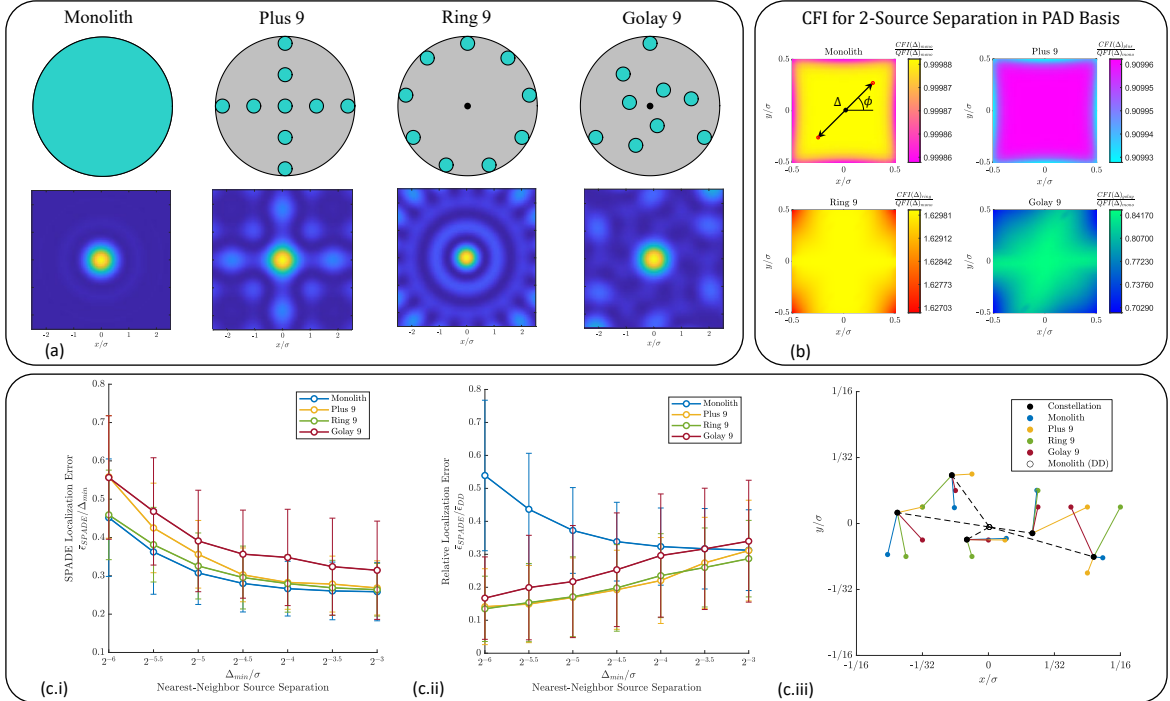
3. Simulation Results

Fig. 1. **(a)** Monolith and 9-aperture systems with diameter ratios $d/D = 1/10$ shown above their respective PSFs. **(b)** Classical Fisher Information (CFI) of the 2-source separation distance Δ measured in the PAD basis as a fraction of the Quantum Fisher Information of the monolithic aperture [3]. **(c.i-ii)** The localization error for modal imaging using different aperture configurations.**(c.iii)** A sample constellations and its modal imaging estimates for all aperture configurations. The meam number of photons per source incident of the effective aperture area was 10^4 and the minimum pairwise separation $\Delta_{min} = \sigma/32$.

We assessed the performance of modal imaging with the multi-aperture configurations depicted in 1(a) using Monte-Carlo simulations. All target constellations were generated as 2D random walks with step size equal to the desired nearest-neighbor separation Δ_{min} between point sources. Across Monte Carlo samples we independently varied the number of point sources, their nearest-neighbor separations, and the Poisson mean for the number of photons per source incident on the effective aperture area. For computational tractability we simulated SPADE measurements on a truncated PAD basis comprised of the first 36 spatial modes. As a general trend, we observe that modal imaging with multi-apertures provides a progressively greater advantage over direct imaging as the estimation task becomes harder (i.e. fewer photons and smaller source separations). In the low-photon $K \sim O(10^3)$ deep sub-Rayleigh $\Delta_{min} < \sigma/16$ regime, modal imaging achieves approximately an order of magnitude reduction in average localization error compared to direct imaging with all three compound aperture configurations.

References

1. M. Tsang, R. Nair, and X.-M. Lu, "Quantum theory of superresolution for two incoherent optical point sources," Phys. Rev. X **6**, 031033 (2016).
2. J. Rehacek, M. Paúr, B. Stoklasa, Z. Hradil, and L. L. Sánchez-Soto, "Optimal measurements for resolution beyond the rayleigh limit," Opt. Lett. **42**, 231–234 (2017).
3. S. Z. Ang, R. Nair, and M. Tsang, "Quantum limit for two-dimensional resolution of two incoherent optical point sources," Phys. Rev. A **95**, 063847 (2017).